PHYSICAL REVIEW A VOLUME 60, NUMBER 3 SEPTEMBER 1999

Near-threshold structures in electron-collision-induced alignment of core-excited atomic states

A. N. Grum-Grzhimailo
Institute of Nuclear Physics, Moscow State University, Moscow 119899, Russia

K. Bartschat
Department of Physics and Astronomy, Drake University, Des Moines, Iowa 50311

B. Feuerstein and W. Mehlhorn
Fakultät für Physik, Universität Freiburg, D-79104 Freiburg, Germany

(Received 14 January 1999)

Structures, likely due to negative-ion resonances, are predicted in the electron-impact-induced alignment of the Na*$(2p^5 3s^2)^2P_{3/2}$ autoionizing state near the excitation threshold. The predictions are supported by measurements of the alignment via the anisotropic emission of the autoionization electrons in the impact energy range from threshold to 80 eV. Our *R*-matrix (close-coupling) calculations successfully reproduce the broad-scale energy dependence of the alignment that, above the resonance region, is found to be similar to that for the valence-excited $(2p^5 3s)^1P_1$ state in Ne. [S1050-2947(99)51109-8]

PACS number(s): 32.80.Fb, 32.80.Hd

Electron-atom collisions between unpolarized beams without detection of the reaction products lead to excited atomic states aligned with respect to the incident electron beam direction. Studies of the collision-induced alignment yield information on the relative excitation cross sections of the magnetic sublevels that is not available from measurements of the total cross sections. The alignment causes a linear polarization of the light emitted in the radiative decay of the excited states. This fluorescence polarization has been of long-term interest for both experiment and theory (see, for example, [1–3], and references therein) and is the major source of information about the collision-induced alignment in noncoincidence experiments. Except for a narrow energy window near the excitation threshold, however, the fluorescence polarization can be strongly influenced by secondary excitation processes, such as cascading, which may contribute substantially already at low impact energies and often become more important as the energy is increased. This effect reduces the benefits of the method to study the direct excitation process and hampers considerably a comparison between calculations of the collision-induced alignment and the experimental results.

In contrast to the frequently studied optical transitions (for recent work, see [4–6]), much less attention has been devoted to the collision-induced alignment of core-excited states that decay nonradiatively via the Coulomb interaction by ejection of an autoionizing electron (see, for example, Matterstock *et al.* [7]). In this case, the angular distribution of the electron emission contains information on the alignment of the decaying state. A major advantage associated with the fast nonradiative decay is the lack of secondary excitation processes contributing to the population of the decaying state. Hence, a direct comparison between theoretical and experimental values of the alignment is possible at essentially arbitrary incident energies. Also, a reduction in the measured alignment due to hyperfine coupling with the nuclear spin, which is of primary importance for the fluorescence depolarization [8], does not have to be considered in excitation autoionization, since the decay time of the autoionizing state is generally much shorter than the precession period due to hyperfine coupling.

For studies of the collision-induced alignment of core-excited states, it is favorable to choose transitions with negligible contribution from direct ionization. In such cases, the two-step excitation-autoionization model provides a valid description and the complexity due to Fano interferences [9,10] can be avoided. Another requirement for a straightforward interpretation of the results is a one-to-one correspondence between the angular distribution of the electron emission and the alignment of the autoionizing state. This is accomplished for nonradiative decay via a single channel, which makes it possible to extract the collision-induced alignment irrespective of the dynamics associated with the autoionization decay. Excitation of the outermost np^6 filled subshell in alkali-metal atoms provides a possibility for carrying out such studies; the direct ionization of the valence $(n+1)s$ electron is negligible in comparison with the resonance ionization via $np^5(n+1)sn'\ell'$ autoionizing states that decay to the ionic ground state $(np^6)^1S_0$.

In this work, we investigate theoretically and experimentally the alignment of the Na$(2p^5 3s^2)^2P_{3/2}$ autoionizing state excited by electrons with energies between threshold (30.77 eV) and 80 eV. Previous investigations found major disagreement between the experimental results for the alignment of the autoionizing state [11] and theoretical predictions based upon first-order plane-wave and distorted-wave methods [12,13]. Consequently, we apply an *R*-matrix (close-coupling) approach to calculate the collision-induced alignment of a core-excited state and apply it to the above transition. Using such a coupled-channel method allows for the detailed investigation of core-excited negative-ion resonances that appear in the near-threshold region.

Details of the theory and the experiment have been published elsewhere [14]. Briefly, the angular anisotropy of the autoionizing electrons from the $^2P_{3/2}$ state as function of the incident electron energy E is given by [15]

$$I_{3/2}(E,\vartheta)=\overline{I}_{3/2}(E)[1+\beta(E)P_2(\cos\vartheta)], \qquad (1)$$

where $\beta(E)=\mathcal{A}_{20}(E)\alpha_2$ is the anisotropy coefficient, $\mathcal{A}_{20}(E)$ and α_2 are the alignment and the decay parameter of the $^2P_{3/2}$ state, respectively, and the ejection angle ϑ is defined relative to the incident electron beam direction. The isotropic part $\overline{I}_{3/2}(E)$ is proportional to the integral excitation cross section of the $^2P_{3/2}$ state, and $\alpha_2=-1$ for the nonradiative decay $^2P_{3/2}\rightarrow{}^1S_0+e^-(p_{3/2})$ [15].

Based upon the Belfast *R*-matrix codes [16], we performed 26-state close-coupling calculations for the transition matrix elements within the *LS*-coupling approximation. States with the following configurations were included in the close-coupling expansion: $(2p^63s)$, $(2p^64s)$, $(2p^65s)$, $(2p^63p)$, $(2p^64p)$, $(2p^63d)$ $(2p^53s^2)$, $(2p^53s3p)$, and $(2p^53s4s)$, together with selected terms of $(2p^53s3d)$ and $(2p^53p^2)$. The *T*-matrix elements for the transition $(2p^63s)^2S\rightarrow(2p^53s^2)^2P$ were then combined to obtain the alignment of the total angular momentum *J* of the autoionizing state as (for atoms with zero orbital momentum in the ground state)

$$\begin{aligned}\mathcal{A}_{20}(J,E)=&(-1)^{J+S}\hat{J}\hat{L}^2\begin{Bmatrix}L & L & 2\\ J & J & S\end{Bmatrix}\\ &\times\left[\sum_{l_0l_1S_t}\hat{S}_t^2\hat{l}_0^2\left|T^{S_t}_{l_0l_1}(E)\right|^2\right]^{-1}\\ &\times\sum_{l_0l_0'l_1S_t}(-1)^{l_1}\hat{S}_t^2\hat{l}_0^2\hat{l}_0'^2(l_00,l_0'0|20)\\ &\times\begin{Bmatrix}L & L & 2\\ l_0 & l_0' & l_1\end{Bmatrix}T^{S_t}_{l_0l_1}(E)T^{S_t*}_{l_0'l_1}(E). \qquad (2)\end{aligned}$$

Here *L* and *S* are the orbital angular momentum and spin of the autoionizing state, l_0 and l_1 are the orbital angular momenta of the incident and scattered electrons, respectively, S_t is the total spin of the scattering channel, and $T^{S_t}_{l_0l_1}(E)$ is the corresponding *T*-matrix element. (In our case, the channel angular momentum L_t and parity are uniquely defined by l_0, and the triangular rule $|l_0-l_1|\leq L\leq l_0+l_1$ must also be satisfied in the denominator.) Furthermore, we abbreviated $\hat{a}\equiv\sqrt{2a+1}$ and used standard notations for the Clebsch-Gordan coefficient and the Wigner $6j$ symbol. For the present case of interest ($L=1$, $S=1/2$, $J=3/2$), Eq. (2) is equivalent to $\mathcal{A}_{20}(J=3/2,E)=(\sigma_{3/2}-\sigma_{1/2})/(\sigma_{3/2}+\sigma_{1/2})$, where σ_M is the angle-integrated excitation cross section for the sublevel with magnetic quantum number *M*. With $L_t\leq12$ and 35 continuum orbitals for each partial wave of the scattered electron, we extended the *R*-matrix calculations up to an incident electron energy of 80 eV. Two sets of target orbitals were used to investigate the sensitivity of the results to the atomic model. The first set consisted of the Clementi-type orbitals given by Msezane and Awuah [17], which we used before in the cross section studies for the transition of interest [18]. The second, purely numerical set, was obtained by a multiconfiguration Hartree-Fock calculation.

The alignment parameter $\mathcal{A}_{20}$ of the Na*$(2p^53s^2)^2P_{3/2}$ autoionizing state was measured via the anisotropic intensity

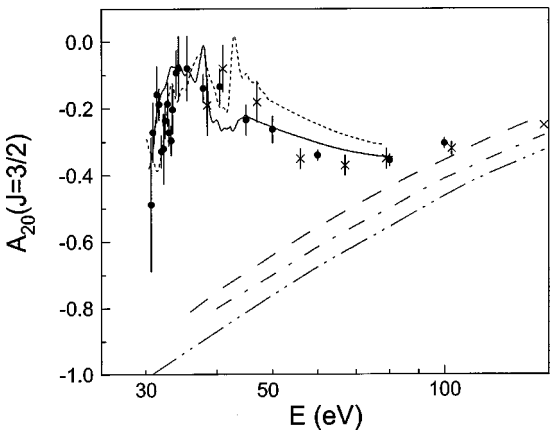

FIG. 1. Alignment of the Na $(2p^53s^2)^2P_{3/2}$ autoionizing state. The solid and short-dashed lines show the *R*-matrix predictions with the Hartree-Fock and Clementi-type electron orbitals, respectively, convoluted with the energy width of the incident beam. The other lines represent previous calculations in the plane-wave and distorted-wave Born approximations (PWBA and DWBA) by Theodosiou [12] (dash-dot-dot) and Pangantiwar and Srivastava [13] (dash-dot, PWBA; dashed, DWBA). The circles represent the present measurements and the stars represent those of DuBois *et al.* [11].

$I_{3/2}(\vartheta)$ of the autoionization electrons according to Eq. (1). In order to eliminate experimental anisotropies we normalized the angle-dependent intensities $I_{3/2}(\vartheta)$ to the intensities $I_{1/2}(\vartheta)$ of the isotropic decay of the $^2P_{1/2}$ state. The fine-structure splitting (0.17 eV) was fully resolved by the apparatus function [40 meV full width at half maximum (FWHM)]. The apparatus used in the present investigation was described in previous publications [19,18]. For emission angles $\vartheta\leq90°$, the intensities $I(\vartheta)$ were measured by rotating the electron gun, whereas a localized magnetic-field method [20] was applied for larger angles. Although the natural width of the autoionization lines is only 3.6 meV, [21] we were able to observe an asymmetry of the line shape due to postcollision interaction [22] at incident electron energies very close to threshold. On the other hand, no effect of Fano interference [9] on the line shape was found even at the lowest energies. From the analysis of the line shapes at these energies we obtained a lower limit for the Fano parameter: $|q|>20$. For each impact energy *E*, the ratio $R(\vartheta)=I_{3/2}(\vartheta)/I_{1/2}(\vartheta)$ was determined for at least three angles ϑ. The alignment parameter $\mathcal{A}_{20}(E)$ was then obtained by fitting an angular distribution according to Eq. (1) to the data for $R(\vartheta)$.

Figure 1 shows our experimental and theoretical results for the alignment of the $(2p^53s^2)^2P_{3/2}$ state of Na at incident energies from threshold to 80 eV (extended to 100 eV in the experiment), i.e., over the energy range in which previous experimental results [11] and calculations [12,13] were in severe disagreement. In this figure, the theoretical curves were convoluted with the experimental energy width (0.75 eV FWHM) of the incident electron beam. Our calculations and measurements are in good overall agreement, although the results are sensitive to the details of the target model. We note that the calculated alignment for energies between 38 eV and 48 eV is (minorly) disturbed by pseudoresonances. Those arise from the fact that only 26 atomic states were

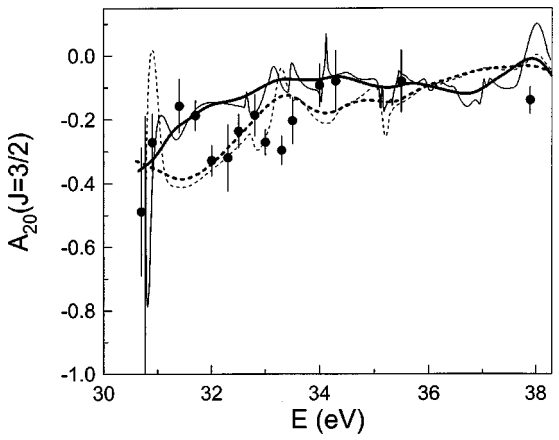

FIG. 2. Same as Fig. 1 in the near-threshold region. The thin and thick lines correspond to the *R*-matrix predictions before and after convolution with the energy width of the electron beam.

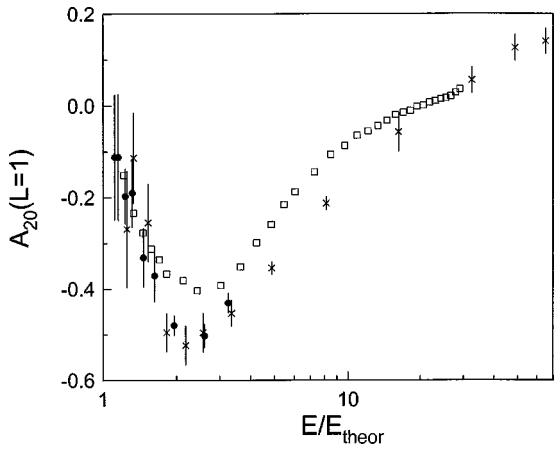

FIG. 3. Orbital angular momentum alignment of the autoionizing $(2p^5 3s^2)^2 P_{3/2}$ state in Na (circles, present data; stars, data of Ref. [11]) and the $(2p^5 3s)^1 P_1$ state of Ne (squares), as evaluated from the linear polarization measurements given in Ref. [23].

included in the close-coupling expansion, while the states themselves were expanded in a more extensive basis set.

Figure 2 displays the near-threshold region where the measured and calculated energy dependence of the alignment indicates the presence of negative-ion resonances, which can be seen very clearly in the calculated curves without convolution. Such resonances in the angle-integrated cross section have been observed and discussed in Ref. [18]. As mentioned above, however, negative-ion resonances in the alignment of core-excited states have not been studied before, in striking contrast to the extensive work on resonances in fluorescence polarization.

Despite the overall satisfactory agreement with each other, the experimental and theoretical results in the resonance region deviate regarding the detailed energy dependence. Searching for an explanation, we checked for a possible influence of the intra-atomic fine-structure interaction. Due to this interaction, negative-ion resonances can be depolarized before the decay, which, in turn, may affect the alignment of the autoionizing state as a product of the resonance decay. We performed a semirelativistic Breit-Pauli *R*-matrix calculation with a more restricted basis of atomic states and found that including the spin-orbit interaction produced only very small changes in the alignment. Even in light of the sensitivity found for the calculated alignment in the near-threshold resonance region, however, the reliability of the present predictions for an autoionizing state is certainly comparable to that obtained for excitation of discrete states [6].

Neither the convoluted curves nor the experimental data in Fig. 2 show the theoretical threshold limit of $\mathcal{A}_{20} = -1$. [This limit follows from Eq. (2) if only the lowest partial wave of the scattered electron is taken into account.] This deviation of observed results from theoretical threshold values is a general feature for situations where the alignment changes rapidly near the excitation threshold, because the energy distribution of the incident electron beam (and thus the convolution integral) averages over the region of sharp variations in the alignment.

Finally, both experiment and theory exhibit a reduction in the absolute value of the alignment as the incident electron energy is decreased from 80 eV, with a minimum of almost zero around 35 eV incident energy (cf. Fig. 1). The plane-wave and distorted-wave Born predictions [12,13] yield good agreement with experiment at energies above 100 eV, but deviate considerably from experiment at lower energies. This points to channel coupling as the reason for the minimum. Similar features in the fluorescence polarization have been observed for many transitions, but the depolarization of the optically decaying state due to cascade population prevents a rigid explanation of such a behavior in optical measurements.

Consequently, it seemed worthwhile to compare the alignment in the orbital angular momentum, $\mathcal{A}_{20}(L)$, for the autoionizing $(2p^5 3s^2)^2 P$ state in sodium and the $(2p^5 3s)^1 P$ discrete state in neon, since these states only differ by one $3s$ electron. For the ^2P state of Na, the orbital angular momentum $\mathcal{A}_{20}(L=1)$ is related to $\mathcal{A}_{20}(J=3/2)$ of the $^2P_{3/2}$ state by $\mathcal{A}_{20}(L=1) = \sqrt{2}\mathcal{A}_{20}(J=3/2)$. To find the alignment for neon we utilize the fluorescence polarization data of Hammond *et al.* [23]. Figure 3 shows the comparison of the alignments as a function of the incident energy (in threshold units) above the region of negative-ion resonances. Since the photons in neon are emitted by the *LSJ*-coupled state $(2p^5 3s)^1 P_1$, the alignment of the orbital angular momentum $\mathcal{A}_{20}(L)$ is related to the fluorescence polarization P by $\mathcal{A}_{20}(L) = 2\sqrt{2}P/(P-3)$. Note, however, that systematic errors can be caused by contributions from unpolarized ion emission lines [23]. In any case, Fig. 3 indicates a striking similarity between the alignment for the two states, despite the cascade effects that are known to influence the measured alignment in neon.

To summarize, we have carried out a combined theoretical and experimental study of the electron-collision-induced alignment of the core-excited $(2p^5 3s^2)^2 P_{3/2}$ state in sodium. *R*-matrix calculations for the alignment of a core-excited state removed a previously existing severe discrepancy between theory and measurements at incident energies below 80 eV. Near-threshold negative-ion resonances in the alignment were predicted theoretically. Although experimental evidence supports the existence of such structures, even more detailed investigations seem necessary before final conclusions can be drawn. Finally, the alignment of the core-excited nonradiatively decaying state exhibits features typical for valence-electron excited states that decay radiatively.

The authors thank O.I. Zatsarinny for assistance in the MCHF structure calculation. This work is part of the joint program ''Dynamics of Autoionizing and Auger States of Alkali Atoms Excited by Electron Impact: Experiment and Theory,'' supported by the Deutsche Forschungsgemeinschaft (DFG) and the Russian Foundation for Basic Research. A.N.G. gratefully acknowledges the hospitality of the Universität Freiburg. This work was also supported, in part, by the DFG via Sonderforschungsbereich 276, by the National Science Foundation under Grant No. PHY-9605124 (K.B.), and by the Foundation ''Universities of Russia'' under Grant No. 5340 (A.N.G.).

[1] H. Kleinpoppen and A. Scharmann, in *Progress in Atomic Spectroscopy. Part A*, edited by W. Hanle and H. Kleinpoppen (Plenum, New York, 1978), p. 329.

[2] D. W. O. Heddle and J. W. Gallagher, Rev. Mod. Phys. **61**, 221 (1989).

[3] G. K. James, J. A. Slevin, D. Dziczek, J. W. McConkey, and I. Bray, Phys. Rev. A **57**, 1787 (1998).

[4] C. Norén, W.L. Karras, J.W. McConkey, and P. Hammond, Phys. Rev. A **54**, 510 (1996), and references therein.

[5] D. H. Yu, P. A. Hayes, J. E. Furst, and J. F. Williams, Phys. Rev. Lett. **78**, 2724 (1997); D. H. Yu, P. A. Hayes, J. F. Williams, and C. Locke, J. Phys. B **30**, L461 (1997), and references therein; D. H. Yu, P. A. Hayes, and J. F. Williams, *ibid.* **30**, L487 (1997).

[6] V. Zeman, K. Bartschat, T. J. Gay, and K. W. Trantham, Phys. Rev. Lett. **79**, 1825 (1997).

[7] B. Matterstock, R. Huster, B. Paripas, A. N. Grum-Grzhimailo, and W. Mehlhorn, J. Phys. B **28**, 4301 (1995).

[8] A. A. Zaidi and H. Kleinpoppen, J. Phys. B **26**, 1669 (1993), and references therein.

[9] U. Fano, Phys. Rev. **124**, 1866 (1961).

[10] V. V. Balashov, S. S. Lipovetsky, and V. S. Senashenko, Zh. Éksp. Teor. Fiz. **63**, 1622 (1972) [Sov. Phys. JETP **36**, 858 (1973)].

[11] R. D. DuBois, L. Mortensen, and M. Rødbro, J. Phys. B **14**, 1613 (1981).

[12] C. E. Theodosiou, Phys. Rev. A **36**, 3138 (1987).

[13] A. W. Pangantiwar and R. Srivastava, J. Phys. B **20**, 5881 (1987).

[14] B. Feuerstein, A. N. Grum-Grzhimailo, K. Bartschat, and W. Mehlhorn, J. Phys. B **32**, 3727 (1999).

[15] E. G. Berezhko and N. M. Kabachnik, J. Phys. B **10**, 2467 (1977); B. Cleff and W. Mehlhorn, *ibid.* **7**, 593 (1974).

[16] K. A. Berrington, W. B. Eissner, and P. H. Norrington, Comput. Phys. Commun. **92**, 290 (1995); V. M. Burke and C. J. Noble, *ibid.* **85**, 471 (1995).

[17] A. Z. Msezane and P. Awuah, J. Phys. B **23**, 4615 (1990).

[18] B. Feuerstein, A. N. Grum-Grzhimailo, and W. Mehlhorn, J. Phys. B **31**, 593 (1998).

[19] W. Weber, R. Huster, M. Kamm, and W. Mehlhorn, Z. Phys. D **22**, 419 (1991).

[20] F. H. Read and J. M. Channing, Rev. Sci. Instrum. **67**, 2372 (1996).

[21] O. I. Zatsarinny and L. A. Bandurina, J. Phys. B **26**, 3765 (1993).

[22] M. Y. Kuchiev and S. A. Sheinerman, J. Phys. B **21**, 2027 (1988), and references therein.

[23] P. Hammond, W. Karras, A. G. McConkey, and J. W. McConkey, Phys. Rev. A **40**, 1804 (1989).